

Revealing Molecular Strong Field Autoionization Dynamics

Sizuo Luo^{1,*}, Jinlei Liu², Xiaokai Li¹, Dongdong Zhang¹, Xitao Yu¹, Dianxiang Ren¹, Mingxuan Li¹, Yizhang Yang¹, Zhenzhen Wang¹, Pan Ma¹, Chuncheng Wang¹, Jing Zhao², Zengxiu Zhao^{2,†} and Dajun Ding^{1,‡}

¹*Institute of Atomic and Molecular Physics, Jilin University, Changchun 130012, China*

²*Department of Physics, National University of Defense Technology, Changsha 410073, China*



(Received 21 September 2020; accepted 5 February 2021; published 12 March 2021)

The novel strong field autoionization (SFAI) dynamics is identified and investigated by channel-resolved angular streaking measurements of two electrons and two ions for the double-ionized CO. Comparing with the laser-assisted autoionization calculations, we demonstrate the electrons from SFAI are generated from the field-induced decay of the autoionizing state with a following acceleration in the laser fields. The energy-dependent photoelectron angular distributions further reveal that the subcycle ac-Stark effect modulates the lifetime of the autoionizing state and controls the emission of SFAI electrons in molecular frame. Our results pave the way to control the emission of resonant high-harmonic generation and trace the electron-electron correlation and electron-nuclear coupling by strong laser fields. The lifetime modulation of quantum systems in the strong laser field has great potential for quantum manipulation of chemical reactions and beyond.

DOI: [10.1103/PhysRevLett.126.103202](https://doi.org/10.1103/PhysRevLett.126.103202)

A quantum system in an excited state with energy higher than ionic states can couple with the ionic states by autoionizing [1]. This is a general phenomenon importantly revealing the electron correlation and electron-nuclear coupling in atoms, molecules, and solids [1–3]. In a field-free condition, the interference between direct ionization and autoionization channels leading to well-known Fano line profiles [1]. When subjected to a laser pulse, the autoionization of atoms and molecules can be modified and the interference can be controlled [4–10]. The coupling between the autoionizing state with other states can be tuned and tracked by adding a weak laser field in the ultrafast measurement [4–6], and the contribution of depletion by strong field ionization (SFI) becomes important as the strength of the laser field increases [7]. Furthermore, the Feshbach resonance enhances the autoionization during the bond breaking of molecules in laser fields [9], where the branching ratios between direct dissociation and autoionization channel can be controlled and the non-Born-Oppenheimer dynamics can be probed by scanning the delay of an infrared (IR) laser [10]. It can be seen that tracing the evolution of molecular autoionizing states with femtosecond or even attosecond resolution can promote the understanding of the electron-electron correlation and electron-nuclear coupling.

Recently, the autoionization dynamics has been traced with the attosecond transient absorption and the attosecond photoelectron measurement in the XUV regime [4–7, 11–15]. In these cases, the IR pulse truncates the autoionizing decay by coupling the autoionizing states to other states (Rydberg state or continuum state) in the range of 10^{11} – 10^{13} W/cm², resulting in a shorter lifetime and a

broader resonance peak [4]. The creation and decay of autoionizing states have been studied in the strong laser fields (10^{13} – 10^{15} W/cm²) interaction with atoms, molecules, and clusters, in which the observed electron spectra are attributed to the field-free decay and electron-nuclear coupling processes [16–18]. The survival of the autoionizing state in strong laser fields can enhance the resonant high-harmonic generation (HHG) [19–22], which presents great potential in composing an intense attosecond XUV pulse [22]. The dynamical Stark effect has been proposed and observed in atoms which not only will shift the resonance of autoionizing states and modify the autoionization decay [4,23], but also can manipulate the spatial-temporal emission of an ultrafast XUV pulse as an opto-optical modulator [24]. In addition, the dynamical Stark effect due to the strong field provides an important approach to the coherent control of photochemical reaction including photodissociation [25] and photoassociation [26]. In this Letter, we demonstrate that the angular-streaking method can be used to identify and probe the SFAI of molecules and show that the instantaneous response of molecules to the laser field due to the ac-Stark effect strongly modifies the decay dynamics of autoionizing states.

Experimentally, we perform the two-electron and two-ion ($2e-2i$) coincident measurements from Coulomb explosion (CE) of CO in strong laser fields by using cold target recoil ion momentum spectroscopy (COLTRIMS) as shown in Fig. 1(a) [27–29]. The laser is positively chirped ($\lambda \sim 800$ nm, 1.1×10^{15} W/cm², ~ 45 fs) to enhance the yield of the autoionization channel and keep the influence of nuclear movement small enough. The chirp-dependent

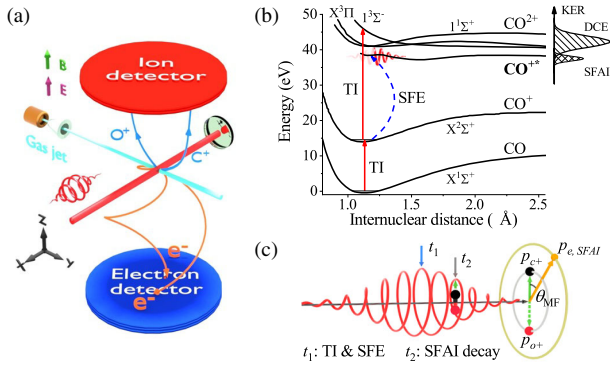


FIG. 1. (a) Schematic diagram of the experimental setup. The yz plane is the polarization plane of the near-circularly polarized pulse. (b) Relevant potential curves, adapted from Refs. [33,38], and the pathways of double ionization including tunneling ionization (TI) and strong field excitation (SFE). The inset shows schematically the KER distributions of the direct Coulomb explosion (DCE) of CO^{2+} and the CE induced by SFAI of CO^{+*} . (c) Process of excitation and field-assisted decay of the autoionizing state as well as the definition of the angle θ_{MF} of the SFAI electron in the molecular frame.

yields can be attributed to the constructive interference between multiphoton excitation channels involving resonantly coupled bound states [30,31] (for details please see the Supplemental Material [32]). The ionization and CE pathways are presented in Fig. 1(b). In the direct CE channel, CO molecules are sequentially double ionized to the dication states followed by CE with a high KER (kinetic energy release). Besides, as shown in Fig. 1(c), CO molecules can also take the pathway followed by tunneling ionization, strong field excitation at t_1 [16,17] and SFAI at t_2 , leading to a lower KER [33–35]. With an anticlockwise near-circularly polarized strong laser field ($\epsilon \sim 0.95$), in this experiment, the angular streaking method is employed to resolve the pathways of two electrons' detachment [36] and to identify the autoionization channels during double ionization of molecules. In this way, the SFAI dynamics at the molecular frame can be traced by mapping the ionization moment in the rotating electric field vector $\{\vec{E}(t) = E_0 f(t) [\hat{y} \sin(\omega t + \phi) + \epsilon \hat{z} \cos(\omega t + \phi)]\}$ to the magnitude and direction of the final momentum of the emitted electron $\vec{p} = p_z \hat{z} + p_y \hat{y}$ [36,37]. Since a multicycle laser pulse is used, the broadband electron spectra [see Fig. 3(b)] result from ionization accumulating for each optical cycles. The subcycle ac Stark effect is traced by analyzing the angular distribution of an electron with a certain energy, i.e., 0° – 360° corresponding to 0–2.67 fs at each laser cycle as shown in Fig. 1(c).

In Fig. 2(a), we show the KER distribution with multiple peaks obtained from CE of different ionic states after double ionization of CO molecules. The channel-resolved sum-momentum distributions of the two ions along the z axis $p_{z,\text{sum}}$ ($p_{z,\text{sum}} = p_{z,C^+} + p_{z,O^+}$) with conditions of C^+

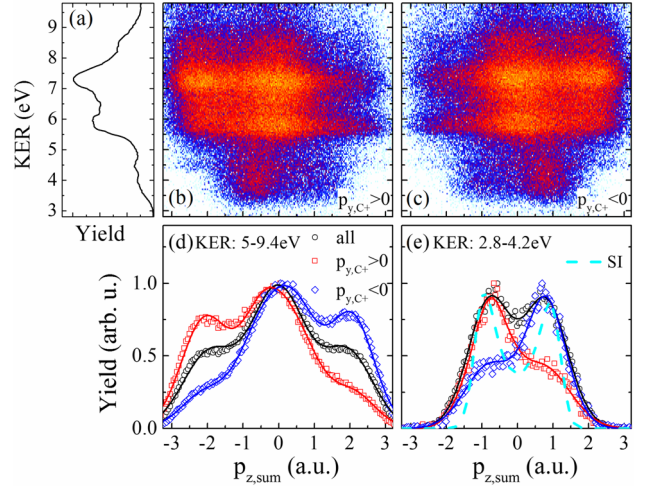


FIG. 2. (a) KER of the $C^+ + O^+$ channel. (b) and (c) KER-dependent ion sum momentum along the z axis ($p_{z,\text{sum}}$) of the $C^+ + O^+$ channel with C^+ emitting along the positive ($p_{y,C^+} > 0$) and negative ($p_{y,C^+} < 0$) direction of the y axis. The corresponding $p_{z,\text{sum}}$ integrated over the KER range 5.0–9.4 eV and 2.8–4.2 eV are plotted in (d),(e). The solid curves are the fits of the measured $p_{z,\text{sum}}$ by considering the convolution of two sequentially emitted electrons. The electron momentum projections on the z axis of single ionization (SI) is also presented as the cyan dashed curve in (e).

emitting to the positive ($p_{y,C^+} > 0$) and negative ($p_{y,C^+} < 0$) directions are present in Figs. 2(b) and 2(c). It can be seen that the $p_{z,\text{sum}}$ shows three-peak distributions for the ions with KER above 5.0 eV from direct CE channels while two-peaks distributions are observed for the ions with KER below 5.0 eV, as shown in Figs. 2(d) and 2(e). The corresponding sum-momentum distribution of electrons can be deduced from that of the ions according to momentum conservation [36,39], i.e., $p_{z,C^+} + p_{z,O^+} + p_{z,e1} + p_{z,e2} \approx 0$. And values $p_{z,e1} = 0.79$ a.u., $p_{z,e2} = 1.32$ a.u. for the electrons are obtained from multi-Gaussian fitting as shown in Fig. 2(d). The asymmetric distribution shown in red and blue lines can be attributed to the direct double ionization from asymmetric orbitals of CO molecules [38–40]. A new channel appears at the KER range of 2.8–4.2 eV, when a positive chirp laser pulse is used. And its yield is sensitive to the chirp of laser (see Supplemental Material [32]). Different from the direct sequential double ionization channels observed previously [39], the $p_{z,\text{sum}}$ has two-peak distributions for ions with KER at 2.8–4.2 eV as shown in Fig. 2(e), from which the peak momenta of $p_{z,e1} = 0.8$ a.u., $p_{z,e2} = 0$ a.u. are obtained from the fitting. The momentum $p_{z,e1}$ is close to the measured momentum of the first electron from sequential double ionization as well as the electron coincident with CO^+ . Thus, the strong asymmetric distributions in the red and blue lines shown in Fig. 2(e) indicates that the first electron is tunnel ionized from the HOMO orbital of CO [41]. Note that the energy range of measured

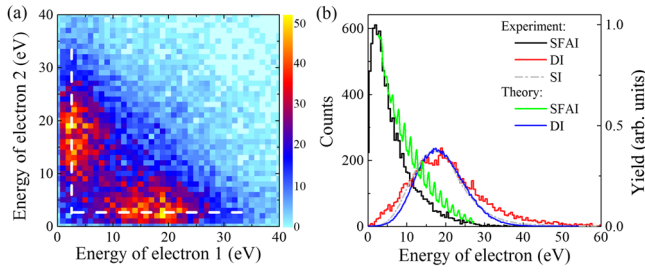


FIG. 3. (a) Electron-electron JES measured in coincidence with the KERs in the range of 2.8–4.2 eV. The plots are symmetrized by switching the energies of two directly measured electrons. (b) Corresponding measured and calculated electron spectra from SFAI. The gray dash-dotted line is the measured electron spectrum from single ionization. Direct ionization (DI) represents the electron spectrum of tunneling ionization from the SFAI related double ionization channel.

KERs at 2.8–4.2 and 4.2–4.8 eV agrees well with the experimental results of XUV induced dissociation from autoionizing states [33–35]. It suggests that the low energy electrons ($p_{z,e2}$ peaks around 0) originate from SFAI of CO^{+*} molecules. And the low-KER CE should be the result of field-induced coupling between autoionizing state and dication state.

In order to investigate the SFAI dynamics, we measure the electron-electron joint energy spectra (JES) from SFAI channel coincident with the low-KER ions (2.8–4.2 eV) in Fig. 3(a). Two successively released electrons are distinguished according to the energy accumulated in the circularly polarized laser field which leads to a crossing distribution of two straight lines (marked by the two dashed white lines). Thus, two sequential released electrons are classified by comparing their final energy, through which the electron with higher energy is assigned to direct ionization and the electron with low energy to SFAI. The electrons from direct tunneling ionization of molecules have a near-Gaussian distribution peaking around 20 eV, as shown by the red line in Fig. 3(b). It agrees well with the electron spectrum coincident with CO^+ obtained from single ionization (gray line), and the distribution is also well reproduced by classical trajectory Monte Carlo (CTMC) calculation (blue line) [42,43]. In contrast, the electrons from SFAI peaks around ~ 1 eV and extends to ~ 30 eV, as shown by the black line in Fig. 3(b). The measured SFAI electron spectrum is different from the single photon induced autoionization in the XUV regime [33], which indicates the autoionization dynamics in the strong laser fields is distinct from that in a field-free condition.

Theoretically, we model the SFAI as a strong field dynamical process with autoionizing state injection and decay (ASID), which is illustrated as three steps: (i) injection: the autoionizing state CO^{+*} is injected when CO molecule being ionized and excited in the strong laser field at t_1 ; (ii) decay: the autoionizing state decays at time t_2 and

the electron is released; (iii) acceleration: the autoionized electron accelerates in the laser fields. Because of significant broadening of the resonance width in the strong field, the effect of nuclear motion on the dynamics of autoionized electrons is negligible (for details please see the Supplemental Material [32]).

Owing to the uncertainty principle, the lifetime τ of the autoionizing state is related to the effective resonance width Γ_{eff} by $\tau = 1/\Gamma_{\text{eff}}$ [44]. Because of the Stark effects in quantum systems with interacting bound and continuum configurations, the characteristic widths of autoionizing resonances can be strongly modified by laser fields [4, 45–47]. When the natural resonance width is much smaller than the Stark broadening under the strong laser fields, the effective resonance width is calculated approximately as

$$\Gamma_{\text{eff}}(t_2) \propto \Delta\mu E(t_2) \cos\beta + \frac{1}{2} \Delta\alpha E(t_2)^2 \cos^2\beta, \quad (1)$$

where β is the angle between the instantaneous direction of the circularly polarized field and molecular axis at t_2 , $\Delta\mu$ and $\Delta\alpha$ are the differences of permanent dipole moment and polarizability tensor components between CO^{+*} and CO^{2+} [48]. Consequently, the Stark effect induces actually a subcycle effect [49]: the resonance width broadens (corresponding to a shorter lifetime) when the electric field vector of the laser is parallel to the direction of the dipole moment, and the width narrows (corresponding to a longer lifetime) when antiparallel. Similarly, the resonance width can be modified by changing the angle between the laser field and molecular axis. With the polarization direction rotating near the peak of the electric field, the lifetime changes from 1 fs to 4 ps in an optical cycle (for details please see Supplemental Material [32]).

The photoelectron spectrum from steps (ii) and (iii) due to decay of the autoionizing state generated at t_1 can be calculated with the improved quantum theory of laser-assisted autoionization [23,50] using

$$b(\vec{p}, t_1) = i \int_{t_1}^{+\infty} e^{-iE_r - [\Gamma_{\text{eff}}(t_2)/2](t_2 - t_1)} e^{-i\Phi_s(t_2)} dt_2, \quad (2)$$

where $\Phi_s(t_2) = \int_{t_2}^{+\infty} \{[\vec{p} - \vec{A}(t_3)]^2/2\} dt_3$ is the quantum phase accumulated in the propagation, E_r is the center energy of the resonance, \vec{p} is the momentum of the electron, and \vec{A} is the vector potential of the laser field. The vector potential \vec{A} is chosen as $\vec{A} = A_0 \cos^2(\pi t/T) [\cos(\omega t)\vec{x} + \sin(\omega t)\vec{y}]$ with $t \in [-T/2, T/2]$ and $T = 90$ fs.

The transient injection of autoionizing states is modeled by treating the CO molecule as an open quantum system [51]. Assuming that the transient injection rate is proportional to the ionization rate of CO, the molecular Ammosov-Delone-Krainov (MO-ADK) theory is employed to obtain the transient injection rate $w_{\text{CO}^{+*}}$ [52,53]. The total yields of SFAI electron is calculated by integrating the weighted photoelectron spectrum with

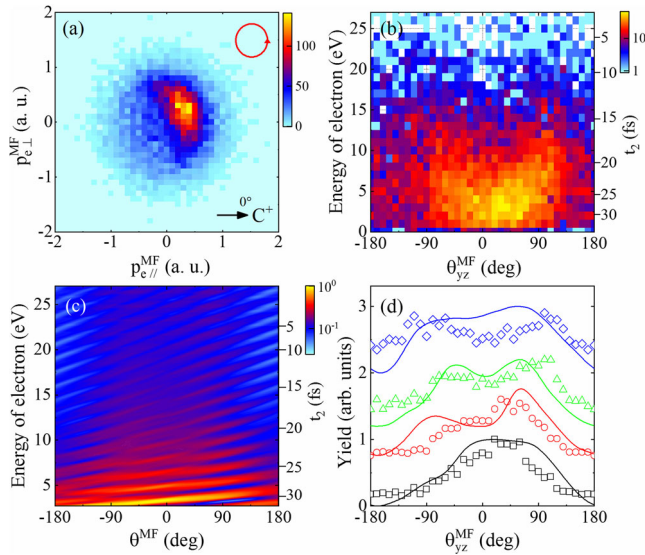


FIG. 4. (a) Molecular frame electron momentum distribution from SFAI in coincidence with CE channels with KERs between 2.8–4.2 eV (with C^+ ions being rotated to 0°). (b),(c) Measured and calculated energy dependent molecular-frame photoelectron angular distributions, (d) the measured and calculated photoelectron angular distributions with the energy at 0–3 eV (black boxes, black line), 3–6 eV (red circles, red line), 6–12 eV (green triangles, green line), and > 12 eV (blue diamonds, blue line).

$Y(\vec{p}) = \int_{-\infty}^{+\infty} |b(\vec{p}, t_1)|^2 w_{CO^{+*}}(t_1) dt_1$. As shown in Fig. 3(b), the calculated electron energy spectrum agrees well with the experimental result. Because of the residual laser field after the autoionization, the SFAI photoelectron spectrum is extended to ~ 30 eV, and discrete peaks separated by one photon energy appear in the calculated energy spectrum reflecting the interaction between the autoionized electron with the laser field [54,55]. The calculation indicates the SFAI occurs in the falling edge of laser pulse and demonstrates that the strong laser field accelerates the decay, reducing the lifetime of the autoionizing state. In this case the SFAI is different from autoionization in the field free condition where the electron emission occurs after the C^+ and O^* are far apart [33,56], and the dissociation time takes more than 250 fs [34]. Furthermore, the measured and calculated electron spectra also differ from the direct tunneling ionization in strong field of circular polarization, which normally show a broad distribution with a single peak far away from zero. The calculation details of the CTMC and ASID models are described in the Supplemental Material [32].

The energy-dependent angular distribution of electron defines the ionization time and reveals the response of autoionizing state to the laser field in a molecular frame, which can be used to trace the subcycle ac-Stark effect on SFAI. Figure 4(a) presents an electron momentum distribution from SFAI in the molecular frame with the C^+ ions directing to 0° . The corresponding measured and calculated energy-dependent angular distributions of electrons are

presented in Figs. 4(b) and 4(c). Assuming the autoionized electron is released on the falling side of the laser envelope, the final energy of the electron can be estimated as $E_f(t_2) = A^2(t_2)/2$ with $t_2 \in [0, T/2]$. Because of the correspondence, the electron released at distinct times t_2 can be mapped to different final energies or momenta in Figs. 4(b) and 4(c). To make the angular distribution clear, we divide the whole energy spectra into four energy intervals as shown in Fig. 4(d). With increasing energy, both the experiment and theory show the angular distributions turn from single peak to double peaks.

It is worth noting that the results calculated by above theoretical model show good agreement with experiment, indicating that the instant ac-Stark effect on the decay of CO^{+*} plays a critical role in the dynamics of SFAI. To clarify the dependence of angular distributions on the electron energy, which is equivalent to the strength of circularly polarized laser field at decay instant, we calculate the SFAI of CO^{+*} without including the permanent dipole moment or polarization in Eq. (1), respectively. As shown in Figs. 5(a) and 5(b), the angular distributions have a single-peak structure when excluding the polarization, while the angular distributions show a double-peak structure when the permanent dipole moment is not included. The results indicate the different decay of the autoionizing state induced by the subcycle responses of permanent dipole moment and polarization. Comparing with the experimental results shown in Fig. 4, different roles of permanent dipole moment and polarization in SFAI can be disentangled in the falling edge of the laser field. The SFAI electron with low energy is released in a weak field (near the end of the laser pulse), where the influence of the permanent dipole moment dominates, leading to the single-peak distributions. In contrast, the influence of polarization dominates when the high energy SFAI electron is released in a strong field (close to the peak of the laser pulse), and a double-peak structure (around $\pm 90^\circ$) of angular distribution appears. In addition, for the energy below ~ 3 eV, the angle of the single peak is distorted strongly by the molecular potential to $\sim 40^\circ$ which is approximately equal to the offset angle at low laser intensity in attoclock measurement [42,57].

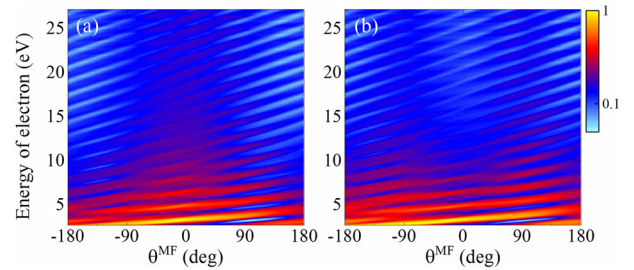


FIG. 5. Energy-dependent photoelectron angular distributions from calculations without (a) polarizability or (b) permanent dipole moment.

The above analyses prove the SFAI occurs in the falling edge of the laser pulse and demonstrate that sub-cycle ac-Stark effect steers the ejection of electrons by modifying the effective resonance width and the lifetime of the autoionizing state, which depends closely on the intensity of the laser field and the angle between the laser field with the molecular axis. For comparison, the energy dependent angular distributions of electrons from SFAI of N_2 are also measured experimentally (see Supplemental Material [32]). Because the N_2 are symmetric molecules without permanent dipole moment, the angular distribution has only a double-peak structure within the whole energy range, which is consistent with the above analysis. Furthermore, the observed strong field induced decay can explain the vanishing of resonant HHG from the autoionizing state in a long IR laser pulse [58], in which the SFAI depletes the population of the autoionizing state at the falling edge of the laser pulse.

In summary, we have investigated the SFAI dynamics of CO^{+*} by coincidentally measuring two electrons and two ions in a circularly polarized strong laser field. The CE processes from the autoionization states have been identified by channel-resolved $p_{z,\text{sum}}$ distributions and electron-electron JES. Both experiment and theory prove the electrons extending from ~ 1 to ~ 30 eV are generated from SFAI. The energy-dependent angular distributions indicate the subcycle ac-Stark effect steers the ejection of electrons by altering the effective resonance width and the lifetime of the autoionizing state in strong laser fields. In addition, we have also observed the SFAI of N_2 and O_2 molecules (see Supplemental Material [32]), proving that the creation and ionization of autoionizing states is a novel but universal phenomenon in strong field physics.

The ability of identifying and tracing the dynamical autoionizing in strong laser fields offers the possibility of disentangling and controlling the ultrafast correlation dynamics in the attosecond timescale. The lifetime modulation of the autoionizing state in strong laser field shows a great potential for manipulating the lifetime of quantum state with tailored strong laser field in many fields, such as the control of resonant HHG [19–22], photodissociation [25], and photoassociation [26].

This work was supported by the National Natural Science Foundation of China (Grants No. 11534004, No. 12074143, No. 11904400, No. 11627807, and No. 12004133), the National Basic Research Program of China (No. 2019YFA0307701 and No. 2019YFA0307703) and the Major Research plan of the National Natural Science Foundation of China (Grant No. 91850201).

S. L., J. L., and X. L. contributed equally to this work.

*luosz@jlu.edu.cn

†zhao.zengxiu@gmail.com

‡dajund@jlu.edu.cn

- [1] U. Fano, *Phys. Rev.* **124**, 1866 (1961).
- [2] S. H. Linn, W. B. Tzeng, J. M. Brom, and C. Y. Ng, *J. Chem. Phys.* **78**, 50 (1983).
- [3] A. E. Miroshnichenko, S. Flach, and Y. S. Kivshar, *Rev. Mod. Phys.* **82**, 2257 (2010).
- [4] H. Wang, M. Chini, S. Chen, C.-H. Zhang, F. He, Y. Cheng, Y. Wu, U. Thumm, and Z. Chang, *Phys. Rev. Lett.* **105**, 143002 (2010).
- [5] S. Gilbertson, M. Chini, X. Feng, S. Khan, Y. Wu, and Z. Chang, *Phys. Rev. Lett.* **105**, 263003 (2010).
- [6] C. Ott, A. Kaldun, P. Raith, K. Meyer, M. Laux, J. Evers, C. H. Keitel, C. H. Greene, and T. Pfeifer, *Science* **340**, 716 (2013).
- [7] A. Kaldun, A. Blättermann, V. Stooß, S. Donsa, H. Wei, R. Pazourek, S. Nagele, C. Ott, C. D. Lin, J. Burgdörfer, and T. Pfeifer, *Science* **354**, 738 (2016).
- [8] M. Eckstein, C.-H. Yang, F. Frassetto, L. Poletto, G. Sansone, M. J. J. Vrakking, and O. Kornilov, *Phys. Rev. Lett.* **116**, 163003 (2016).
- [9] A. S. Sandhu, E. Gagnon, R. Santra, V. Sharma, W. Li, P. Ho, P. Ranitovic, C. L. Cocke, M. M. Murnane, and H. C. Kapteyn, *Science* **322**, 1081 (2008).
- [10] X. Zhou, P. Ranitovic, C. W. Hogle, J. H. D. Eland, H. C. Kapteyn, and M. M. Murnane, *Nat. Phys.* **8**, 232 (2012).
- [11] C. Ott, A. Kaldun, L. Argenti, P. Raith, K. Meyer, M. Laux, Y. Zhang, A. Blättermann, S. Hagstötz, T. Ding, R. Heck, J. Madroño, F. Martín, and T. Pfeifer, *Nature (London)* **516**, 374 (2014).
- [12] V. Gruson, L. Barreau, Á. Jiménez-Galan, F. Risoud, J. Caillat, A. Maquet, B. Carré, F. Lepetit, J. F. Hergott, T. Ruchon, L. Argenti, R. Taïeb, F. Martín, and P. Salières, *Science* **354**, 734 (2016).
- [13] C. Cirelli, C. Marante, S. Heuser, C. L. M. Petersson, Á. J. Galán, L. Argenti, S. Zhong, D. Busto, M. Isinger, S. Nandi, S. Maclot, L. Rading, P. Johnsson, M. Gisselbrecht, M. Lucchini, L. Gallmann, J. M. Dahlström, E. Lindroth, A. L’Huillier, F. Martín, and U. Keller, *Nat. Commun.* **9**, 955 (2018).
- [14] L. Argenti and E. Lindroth, *Phys. Rev. Lett.* **105**, 053002 (2010).
- [15] J. Zhao and M. Lein, *New J. Phys.* **14**, 065003 (2012).
- [16] L. Fechner, N. Camus, A. Krupp, J. Ullrich, T. Pfeifer, and R. Moshhammer, *Phys. Rev. A* **92**, 051403(R) (2015).
- [17] Y. Mi, N. Camus, L. Fechner, M. Laux, R. Moshhammer, and T. Pfeifer, *Phys. Rev. Lett.* **118**, 183201 (2017).
- [18] B. Schütte, J. Lahl, T. Oelze, M. Krikunova, M. J. J. Vrakking, and A. Rouzée, *Phys. Rev. Lett.* **114**, 123002 (2015).
- [19] V. Strelkov, *Phys. Rev. Lett.* **104**, 123901 (2010).
- [20] J. Rothhardt, S. Hädrich, S. Demmler, M. Krebs, S. Fritzsche, J. Limpert, and A. Tünnermann, *Phys. Rev. Lett.* **112**, 233002 (2014).
- [21] N. Rosenthal and G. Marcus, *Phys. Rev. Lett.* **115**, 133901 (2015).
- [22] M. A. Fareed, V. V. Strelkov, N. Thiré, S. Mondal, B. E. Schmidt, F. Légaré, and T. Ozaki, *Nat. Commun.* **8**, 16061 (2017).
- [23] M. Wickenhauser, J. Burgdörfer, F. Krausz, and M. Drescher, *Phys. Rev. Lett.* **94**, 023002 (2005).
- [24] S. Bengtsson, E. W. Larsen, D. Kroon, S. Camp, M. Miranda, C. L. Arnold, A. L’Huillier, K. J. Schafer,

- M. B. Gaarde, L. Rippe, and J. Mauritsson, *Nat. Photonics* **11**, 252 (2017).
- [25] B. J. Sussman, D. Townsend, M. Yu. Ivanov, and A. Stolow, *Science* **314**, 278 (2006).
- [26] L. Levin, W. Skomorowski, L. Rybak, R. Kosloff, C. P. Koch, and Z. Amitay, *Phys. Rev. Lett.* **114**, 233003 (2015).
- [27] R. Dörner, V. Mergel, O. Jagutzki, L. Spielberger, J. Ullrich, R. Moshhammer, and H. Schmidt-Böcking, *Phys. Rep.* **330**, 95 (2000).
- [28] J. Ullrich, R. Moshhammer, A. Dorn, R. Dörner, L. P. H. Schmidt, and H. Schmidt-Böcking, *Rep. Prog. Phys.* **66**, 1463 (2003).
- [29] C. Wang, X. Li, X.-R. Xiao, Y. Yang, S. Luo, X. Yu, X. Xu, L.-Y. Peng, Q. Gong, and D. Ding, *Phys. Rev. Lett.* **122**, 013203 (2019).
- [30] U. Saalmann, S. K. Giri, and J. M. Rost, *Phys. Rev. Lett.* **121**, 153203 (2018).
- [31] M. Kübel, M. Spanner, Z. Dube, A. Yu. Naumov, S. Chelkowski, A. D. Bandrauk, M. J. J. Vrakking, P. B. Corkum, D. M. Villeneuve, and A. Staudte, *Nat. Commun.* **11**, 2596 (2020).
- [32] See Supplemental Material at <http://link.aps.org/supplemental/10.1103/PhysRevLett.126.103202> for more details on the experimental setup, additional experimental data and theoretical calculations including the CTMC and ASID models.
- [33] T. Osipov, T. Weber, T. N. Rescigno, S. Y. Lee, A. E. Orel, M. Schöffler, F. P. Sturm, S. Schössler, U. Lenz, T. Havermeier, M. Kühnel, T. Jahnke, J. B. Williams, D. Ray, A. Landers, R. Dörner, and A. Belkacem, *Phys. Rev. A* **81**, 011402(R) (2010).
- [34] W. Cao, S. De, K. P. Singh, S. Chen, M. S. Schöffler, A. S. Alnaser, I. A. Bocharova, G. Laurent, D. Ray, S. Zhrebtsov, M. F. Kling, I. Ben-Itzhak, I. V. Litvinyuk, A. Belkacem, T. Osipov, T. Rescigno, and C. L. Cocke, *Phys. Rev. A* **82**, 043410 (2010).
- [35] S. Hsieh and J. H. D. Eland, *J. Phys. B* **29**, 5795 (1996).
- [36] A. N. Pfeiffer, C. Cirelli, M. Smolarski, R. Dörner, and U. Keller, *Nat. Phys.* **7**, 428 (2011).
- [37] P. Eckle, M. Smolarski, P. Schlup, J. Biegert, A. Staudte, M. Schöffler, H. G. Muller, R. Dörner, and U. Keller, *Nat. Phys.* **4**, 565 (2008).
- [38] A. Pandey, B. Bapat, and K. R. Shamasundar, *J. Chem. Phys.* **140**, 034319 (2014).
- [39] J. Wu, L. P. H. Schmidt, M. Kunitski, M. Meckel, S. Voss, H. Sann, H. Kim, T. Jahnke, A. Czasch, and R. Dörner, *Phys. Rev. Lett.* **108**, 183001 (2012).
- [40] X. Li, J. Yu, H. Xu, X. Yu, Y. Yang, Z. Wang, P. Ma, C. Wang, F. Guo, Y. Yang, S. Luo, and D. Ding, *Phys. Rev. A* **100**, 013415 (2019).
- [41] B. Zhang, J. Yuan, and Z. Zhao, *Phys. Rev. Lett.* **111**, 163001 (2013).
- [42] J. Liu, Y. Fu, W. Chen, Z. Lü, J. Zhao, J. Yuan, and Z. Zhao, *J. Phys. B* **50**, 055602 (2017).
- [43] J. Liu, J. Zhao, Y. Huang, X. Wang, and Z. Zhao, *Phys. Rev. A* **102**, 023109 (2020).
- [44] L. Medišauskas, F. Morales, A. Palacios, A. González-Castrillo, L. Plimak, O. Smirnova, F. Martín, and M. Y. Ivanov, *New J. Phys.* **17**, 053011 (2015).
- [45] R. R. Freeman and G. C. Bjorklund, *Phys. Rev. Lett.* **40**, 118 (1978).
- [46] D. E. Kelleher, J. F. Delpéch, and J. Weiner, *Phys. Rev. A* **32**, 2230 (1985).
- [47] M. Chini, X. Wang, Y. Cheng, Y. Wu, D. Zhao, D. A. Telnov, S.-I. Chu, and Z. Chang, *Sci. Rep.* **3**, 1105 (2013).
- [48] L. Holmegaard, J. L. Hansen, L. Kalhøj, S. Louise Kragh, H. Stapelfeldt, F. Filsinger, J. Küpper, G. Meijer, D. Dimitrovski, M. Abu-samaha, C. P. J. Martiny, and L. Bojer Madsen, *Nat. Phys.* **6**, 428 (2010).
- [49] M. Chini, B. Zhao, H. Wang, Y. Cheng, S. X. Hu, and Z. Chang, *Phys. Rev. Lett.* **109**, 073601 (2012).
- [50] Z. X. Zhao and C. D. Lin, *Phys. Rev. A* **71**, 060702(R) (2005).
- [51] Q. Zhang, H. Xie, G. Li, X. Wang, H. Lei, J. Zhao, Z. Chen, J. Yao, Y. Cheng, and Z. Zhao, *Commun. Phys.* **3**, 50 (2020).
- [52] X. M. Tong, Z. X. Zhao, and C. D. Lin, *Phys. Rev. A* **66**, 033402 (2002).
- [53] X. M. Tong and C. D. Lin, *J. Phys. B* **38**, 2593 (2005).
- [54] K. J. Schafer, B. Yang, L. F. DiMauro, and K. C. Kulander, *Phys. Rev. Lett.* **70**, 1599 (1993).
- [55] K.-J. Yuan and A. D. Bandrauk, *Phys. Rev. A* **84**, 013426 (2011).
- [56] Y. Hikosaka and J. H. D. Eland, *Chem. Phys.* **299**, 147 (2004).
- [57] A. W. Bray, S. Eckart, and A. S. Kheifets, *Phys. Rev. Lett.* **121**, 123201 (2018).
- [58] M. A. Fareed, V. V. Strelkov, M. Singh, N. Thiré, S. Mondal, B. E. Schmidt, F. Légaré, and T. Ozaki, *Phys. Rev. Lett.* **121**, 023201 (2018).